

Marquette University

e-Publications@Marquette

Physics Faculty Research and Publications

Physics, Department of

7-1999

1-Butaneboronic Acid Binding to *Aeromonas proteolytica* Aminopeptidase: A Case of Arrested Development

Carin C. De Paola
Brandeis University


Brian Bennett
Marquette University, brian.bennett@marquette.edu

Richard C. Holz
Marquette University, richard.holz@marquette.edu

Dagmar Ringe
Brandeis University

Gregory A. Petsko
Brandeis University

Follow this and additional works at: https://epublications.marquette.edu/physics_fac

 Part of the [Physics Commons](#)

Recommended Citation

De Paola, Carin C.; Bennett, Brian; Holz, Richard C.; Ringe, Dagmar; and Petsko, Gregory A., "1-Butaneboronic Acid Binding to *Aeromonas proteolytica* Aminopeptidase: A Case of Arrested Development" (1999). *Physics Faculty Research and Publications*. 52.
https://epublications.marquette.edu/physics_fac/52

Marquette University

e-Publications@Marquette

Physics Faculty Research and Publications/College of Arts and Sciences

This paper is NOT THE PUBLISHED VERSION; but the author's final, peer-reviewed manuscript. The published version may be accessed by following the link in the citation below.

Biochemistry, Vol. 38, No. 28 (1 July 1999): 9048–9053. [DOI](#). This article is © American Chemical Society Publications and permission has been granted for this version to appear in [e-Publications@Marquette](#). American Chemical Society Publications does not grant permission for this article to be further copied/distributed or hosted elsewhere without the express permission from American Chemical Society Publications.

1-Butaneboronic Acid Binding to *Aeromonas proteolytica* Aminopeptidase: A Case of Arrested Development

Carin C. De Paola

The Rosenstiel Basic Medical Sciences Research Center, Brandeis University, Waltham, Massachusetts

Brian Bennett

Department of Chemistry and Biochemistry, Utah State University, Logan, Utah

Richard C. Holz

Department of Chemistry and Biochemistry, Utah State University, Logan, Utah

Dagmar Ringe

The Rosenstiel Basic Medical Sciences Research Center, Brandeis University, Waltham, Massachusetts

Departments of Biochemistry and Chemistry and the Rosenstiel Basic Medical Sciences Research Center, Brandeis University Waltham, Massachusetts

Gregory A. Petsko

The Rosenstiel Basic Medical Sciences Research Center, Brandeis University, Waltham, Massachusetts

Departments of Biochemistry and Chemistry and the Rosenstiel Basic Medical Sciences Research Center, Brandeis University Waltham, Massachusetts

SUBJECTS:

Inhibitors, Peptides and proteins, Metals, Transition states, Ions

Abstract

Hydrolases containing two metal ions connected by a bridging ligand catalyze reactions important in carcinogenesis, tissue repair, post-translational modification, control and regulation of biochemical pathways, and protein degradation. The aminopeptidase from *Aeromonas proteolytica* serves as a paradigm for the study of such bridged bimetallic proteases since its three-dimensional structure is known to very high resolution and its catalytic reaction is amenable to spectroscopic examination. Herein, we report the X-ray crystal structure at 1.9 Å resolution of AAP complexed with 1-butaneboronic acid (BuBA). This structure suggests that this complex represents a snapshot of the proteolytic reaction in an arrested form between the Michaelis complex and the transition state. Comparison of the structure with spectroscopic and other data allows us to conclude that the apparently structurally symmetrical dizinc site is actually asymmetric electrostatically.

This work was supported by the National Science Foundation (CHE-9816487 to RCH), by the National Institutes of Health (GM26788 to GAP and DR), and, in part, by the Macromolecular Structure and Mechanisms Training Grant from the NIH (CCD).

Hydrolases that contain two metal ions connected by a bridging ligand catalyze such diverse reactions as the degradation of DNA, RNA, phospholipids, and polypeptides (1–4). They are, therefore, key players in carcinogenesis, tissue repair, protein maturation, hormone-level regulation, cell-cycle control, and protein degradation processes. In addition, binuclear metallohydrolases are involved in the degradation of agricultural neurotoxins, urea, antibiotics, and several phosphorus(V) materials used in chemical weaponry (5–7). These enzymes use different metal ion Lewis acidities in discrete binuclear sites to (1) bind and position substrate, (2) bind and activate a water molecule to yield an active site hydroxide nucleophile, and/or (3) stabilize the transition state of the hydrolytic reaction. Despite their ubiquity and the considerable structural information available, little is known about how bridged bimetallic centers function during catalytic turnover.

The binuclear metallo-aminopeptidases catalyze the hydrolysis of N-terminal amino acid residues from proteins and polypeptides and are typically grouped into two distinct subclasses: those that are capable of removing nearly any amino acid from the N-terminus of a polypeptide chain and those that selectively remove methionine (8–10). All of these enzymes are widely distributed in bacteria, yeast, plant, and animal tissues (10). Abnormal aminopeptidase activity has been associated with many health conditions and pathologies, including aging, cataracts, inflammation, cystic fibrosis, cancer, and leukemia; thus, their biological and medicinal significance is immense (8–10). For example, the naturally occurring peptide-analogue inhibitor, bestatin, was recently shown to significantly decrease HIV infection in males by inhibiting leucine aminopeptidase activity (11). Moreover, a recent study has shown that several naturally occurring aminopeptidase inhibitors (i.e., bestatin, leuhistin, and actinonin) inhibit matrix degradation and invasion of extracellular matrixes by fibrosarcoma cells (12). Thus, the inhibition of aminopeptidase activity at malignant tumors is critically important in preventing the growth and proliferation of cancer. This fact is underscored by the recent observation that the eukaryotic binuclear

metallohydrolase methionine aminopeptidase II is the target for the antitumor drugs ovalicin and fumagillin (13, 14).

The dizinc aminopeptidase from *Aeromonas proteolytica* (AAP) is a small, monomeric enzyme (32 000 Da), thermostable for several hours at 70 °C, that has been previously crystallographically characterized (15, 16). AAP possesses a (μ -aqua)(μ -carboxylato)dizinc(II) core with a terminal carboxylate and histidine residue at each metal (Figure 1). Both Zn(II) ions in AAP have a distorted tetrahedral coordination geometry with a Zn–Zn distance of 3.5 Å. The X-ray crystal structure of AAP complexed to the transition state analogue inhibitor d-iodophenylalanine hydroxamate shows that a single oxygen atom of the hydroxamate inhibitor bridges between the two active-site Zn(II) ions with the concomitant loss of the bridging water molecule (16). This structure is similar to the transition state analogue inhibited structures of bovine lens aminopeptidase (bLAP) complexed with l-leucinal and l-leucine phosphonic acid (LPA) (17, 18) and AAP bound by LPA (19). These structures of transition state analogue complexes have been interpreted as representing one stage of the reaction mechanism.

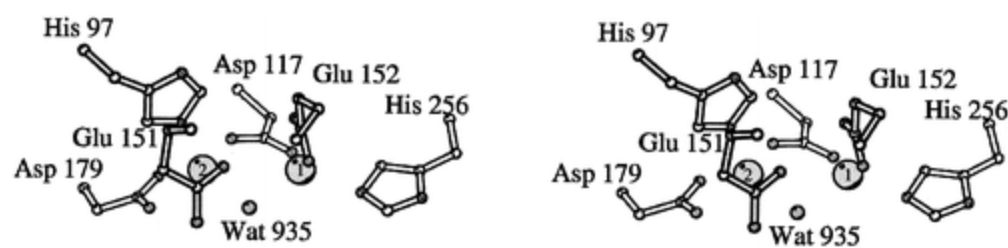


Figure 1 Stereoimage of the native AAP active site calculated from coordinates 1AMP, (15). The zinc ions of the binuclear center have symmetric coordination spheres in that each has a terminal carboxylate and histidine residue in addition to the bridging aspartate and water molecule. Glu151, also shown, is not a metal ligand but is thought to participate in the hydrolytic reaction.

Herein, we present the X-ray crystal structure, at 1.9 Å resolution, of AAP coordinated by the competitive inhibitor 1-butaneboronic acid (BuBA). Comparison of this structure with spectroscopic and X-ray crystallographic data from the binding of both substrate and transition state analogues of peptide hydrolysis reveals that the BuBA complex represents a snapshot of the proteolytic reaction in an arrested form between the Michaelis complex and the transition state. Combination of these data with previously reported spectroscopic and X-ray crystallographic data have allowed a detailed mechanism of action to be proposed for the metal-mediated peptide hydrolysis reaction catalyzed by AAP.

Materials and Methods

Purification of AAP.

All chemicals used in this study were purchased commercially and of the highest quality available. The AAP was purified from a stock culture kindly provided by Professor Céline Schalk. Cultures were grown according to the previously published procedure (20) with minor modifications to the growth media (21). Purified enzyme was stored at –80 °C until needed.

Spectrophotometric Assay of AAP.

AAP activity was measured by the method of Prescott and Wilkes (22) as modified by Baker et al. (23). In this assay, the hydrolysis of 0.5 mM l-leucine-*p*-nitroanilide (10 mM Tricine, pH 8.0, containing 0.1 mM ZnSO₄) was measured spectrophotometrically at 25 °C by monitoring the formation of *p*-nitroaniline. The extent of hydrolysis was calculated by monitoring the increase in absorbance at 405 nm ($\Delta\epsilon_{405}$ value of *p*-nitroaniline of 10 800 M⁻¹ cm⁻¹) (23). One unit was defined as the amount of enzyme that releases 1 μmol of *p*-nitroaniline at 25

°C in 60 s. The specific activity of purified AAP was typically found to be 120 units/mg of enzyme. This value is identical to that reported by Prescott and Wilkes (20). All spectrophotometric assays were performed on a Shimadzu UV-3101PC spectrophotometer equipped with a constant temperature cell holder. Enzyme concentrations were determined from the absorbance at 278 nm with the value $\epsilon_{278} = 41\,800\text{ M}^{-1}\text{ cm}^{-1}$ (24).

Crystallization, Data Collection, and Processing.

AAP was cocrystallized with BuBA using the crystallization conditions reported for the native enzyme (25), following preincubation with a 4-fold molar excess of BuBA. The purified AAP ($10\text{ mg}\cdot\text{mL}^{-1}$) in 10 mM Tris at pH 8.0, 10 mM KSCN, 0.4 M NaCl, and 4-fold molar excess of BuBA was crystallized by vapor diffusion using 100 mM Tris at pH 8.0, 100 mM KSCN, and 4.5 M NaCl as the precipitating solution. Crystals with dimensions $0.7 \times 0.4 \times 0.4\text{ mm}^3$ were obtained in 2 days and were shown to be isomorphous with the native crystals.

Diffraction data were collected at 4 °C on an *R*-axis IIC Image plate area detector system mounted on a Rigaku RU-200B rotating anode generator, operating at 45 kV and 130 mA. A 0.5 mm collimator was used, and the crystal to detector distance was 100 mm. One crystal was used with one orientation, but the oscillation step size was changed from 1 to 0.5 deg before completing the data collection. The data were processed using XDS97 (26). The data processing and refinement statistics are outlined in Table 1. The overall completeness of 84% was lowered by the completeness of the outermost shell. In the outermost shell (2.1–1.9 Å), the completeness was only 46.7%, whereas the completeness in the next resolution shell (2.3–2.1 Å) was 93%. The R_{merge} in this outermost shell was 37.8%, resulting in an overall R_{merge} (on *I*) of 13.4%, including these data. Ultimately, the decision to keep all of the data to 1.9 Å was based on the quality of the electron density maps where these data were included.

Table 1: Data Collection and Refinement Statistics

Crystal Data	
space group	P6 ₁ 22
unit cell parameters (Å)	
<i>a</i>	109.2
<i>b</i>	109.2
<i>c</i>	97.7
Data Processing	
no. of reflections, observed	163 530
no. of reflections, unique	23 658
cutoff (<i>I</i> /σ)	0
R_{merge}^a (overall) (%)	13.4
completeness, overall (%)	84.2
highest resolution shell (Å)	1.9–2.1
completeness, outer shell (%)	46.7
Model Refinement	
resolution range (Å)	10–1.9
cutoff (<i>F</i> /σ <i>F</i>)	0
R-factor ^b (%)	19.3
no. of reflections	21 322
R_{free} (%)	22.9
no. of reflections	2336
no. of protein atoms	2211
no. of zinc ions	2
no. of BuBA atoms	6

no. of water molecules	134
<i>B</i> -factor model	individual
rmsd from ideality	
bond lengths (Å)	0.006
bond angles (deg)	1.16
improper angles (deg)	0.61
dihedral angles (deg)	25.8
residues in most favored positions ^c (%)	87.2

^a $R_{\text{merge}} = \sum |I_{\text{obs}} - I_{\text{avg}}| / \sum I_{\text{avg}}$. ^b $R\text{-factor} = \sum |F_{\text{obs}} - F_{\text{calc}}| / \sum |F_{\text{obs}}|$. ^c As determined by the program PROCHECK.

Structure Solution and Refinement. Since the crystal of the BuBA-inhibited enzyme was isomorphous with that of the native enzyme, the phases from the published native structure (1AMP, ref 15) were used as the starting model (15). In this process, the zinc atoms and water molecules were omitted from the original coordinate file. All refinement procedures were carried out using the software package X-PLOR (27), and the initial model was subjected to a rigid body refinement using reflections in the 20–4.0 Å resolution range. Subsequent rounds of positional refinement were carried out using higher resolution data incrementally to 1.9 Å resolution. The *R*-factor and *R*-free (28) at this point were 0.27 and 0.31, respectively. Difference electron density maps with coefficients $2F_{\text{obs}} - F_{\text{calc}}$ and $F_{\text{obs}} - F_{\text{calc}}$ (29, 30) were then calculated; these showed clear electron density in the active site for the missing zinc atoms as well as bound inhibitor and a water molecule in close proximity to the bound inhibitor. The two zinc ions and several water molecules were added, and the model was subjected to further rounds of positional refinement. To avoid any bias toward the form of the inhibitor during refinement of the structure, the inhibitor was not yet built into the electron density. Only after several more rounds of refinement and the addition of more water molecules were the coordinates for BuBA built into the electron density. A model for BuBA was built using QUANTA (Molecular Simulations, Inc.) in an almost pyramidal arrangement. This model of BuBA was fitted into the observed electron density in a form having only two oxygen ligands. This electron density showed no sign of a third oxygen atom attached to the boron atom. Because the density at the boron atom was clearly not planar, the parameter files for the inhibitor were edited such that the constraints placed on all angles within the inhibitor were relaxed during refinement. Without relaxing these constraints, the inhibitor was not able to fit the electron density accurately.

An attempt was made to build into the electron density a form of the inhibitor having three oxygen atoms around the boron atom, despite the lack of visible electron density for the third oxygen. This was impossible, however, because of the extremely close proximity of water-53. The distance between this water molecule and the putative third oxygen atom was only 1.1 Å. This information combined with the lack of electron density for a third oxygen caused us to build the inhibitor with only two oxygen atoms. To be sure that the distance between the boron atom and water-53 was not due to deficiencies in the parameters used, the structure was also subjected to a refinement protocol in which all van der Waals and electrostatic interaction terms between water-53 and BuBA were turned off. The distance between water-53 and the boron atom remained unchanged after such refinement.

The electron density for the inhibitor did not extend to the last carbon of BuBA, and this carbon was, therefore, not built into the structure. Further rounds of positional refinement as well as overall and individual *B*-factor refinement resulted in a final structure with an *R*-factor of 0.19 and an *R*-free of 0.23. At this resolution the anticipated error in the coordinate positions is 0.1–0.2 Å. In addition to the 291 amino acid residues, the final model contains 2 zinc ions, 134 water molecules, and 6 atoms of the inhibitor molecule. The terminal carbon of BuBA was omitted due to lack of electron density. Simulated annealing omit maps, in which the active site region was omitted, were calculated and confirmed the presence and the geometry of the bound inhibitor and water-53.

Results and Discussion

Spectroscopic and crystallographic studies on aminopeptidases, to date, have focused on the native enzymes and analogues of the tetrahedral transition state of peptide hydrolysis. These include studies on transition state analogue complexes of both bovine lens leucine aminopeptidase (bLAP) and AAP, which have been interpreted in terms of various catalytic steps (16–18, 31, 32). For AAP, kinetic, optical, and EPR data on the binding of L-leucinephosphonic acid (LPA) to the dicobalt(II)-substituted ([CoCo(AAP)]) enzyme and the heterobimetallic ([CoZn(AAP)] and [ZnCo(AAP)]) enzymes suggested that a single oxygen atom bridge *is not* present in this complex (19). Since LPA was shown to interact with both metal centers, LPA was proposed to bind to the binuclear cluster of AAP as an η -1,2- μ -phosphonate with one of the ligands at the second divalent metal ion provided by the N-terminal amine. The proposed structure for LPA binding is consistent with preliminary X-ray crystallographic data for [ZnZn(AAP)] bound by LPA (De Paola, unpublished results). The X-ray crystal structure of the transition state analogue inhibitor d-iodophenylalanine hydroxamate bound to AAP also indicated both metal ions are involved in binding the inhibitor (16). Similarly, X-ray crystal structures of bLAP with the transition state analogue inhibitors LPA and L-leucine bound to the binuclear Zn(II) cluster show that both inhibitors provide a single oxygen atom bridge between the two Zn(II) ions (17, 18). These data suggest that in the transition state of peptide hydrolysis, both metal ions are involved in coordinating the tetrahedral intermediate.

A mechanism was proposed for bLAP in which both active site metal ions function as Lewis acids (18). In this mechanism, a bridging hydroxide ion acts as the nucleophile by attacking the scissile carbonyl carbon of the peptide substrate. However, for AAP, a mechanism like that of thermolysin or carboxypeptidase A was proposed on the basis of an active-site carboxylate that forms a hydrogen bond to the bridging oxygen atom of the inhibitor d-iodophenylalanine hydroxamate (16, 31, 32). These structures of transition state analogue complexes have been interpreted as representing one stage of the reaction mechanism. Consequently, a number of aspects of the hydrolytic chemistry catalyzed by the binuclear metal clusters of aminopeptidases have gone unexplored. To examine the interactions of an AAP complex representing an earlier stage of the reaction, we have crystallized AAP in the presence of the putative substrate analogue inhibitor 1-butaneboronic acid (BuBA). The structure of the AAP–BuBA complex has been determined to 1.9 Å resolution (Figure 2).

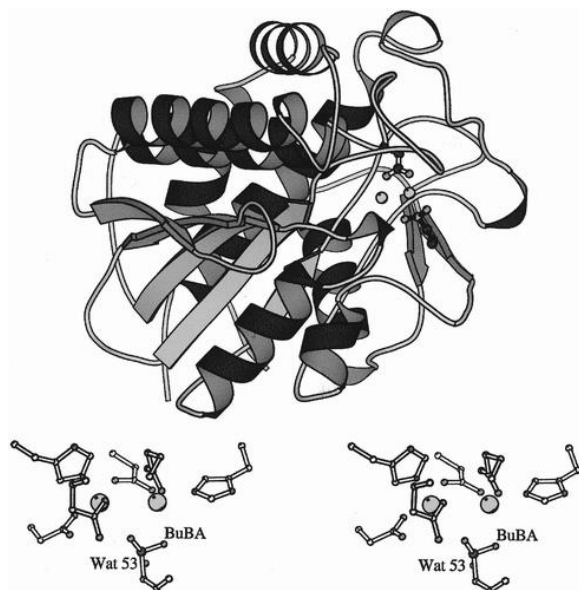


Figure 2 Ribbon diagram of the X-ray crystal structure of AAP complexed with 1-butaneboronic acid (BuBA) (top). The two zinc(II) ions are depicted as gray spheres. The bridging Asp117 is also shown. Stereoimage of the

AAP–BuBA complex active site (bottom). BuBA is bound asymmetrically with respect to the zinc ions. In this view, water-53 is located behind BuBA.

Boronic acids have been reported to be competitive, slow-binding inhibitors of aminopeptidases. For instance, α -aminoboronic acids are known to be biphasic slow-binding aminopeptidase inhibitors (33). The boronic acid BuBA ($K_i = 10 \mu\text{M}$ at pH 8.0) (34) binding to AAP has been previously studied by probing the [CoCo(AAP)], [CoZn(AAP)], and [ZnCo(AAP)] enzyme–complexes by EPR spectroscopy (35, 36). The addition of BuBA to [CoZn(AAP)] resulted in a distinct change in the EPR spectrum; however, addition of BuBA to [ZnCo(AAP)] left the EPR spectrum completely unperturbed. These data are similar to those obtained from electronic absorption spectroscopy (37) and indicate that BuBA binds only to the first metal binding site of AAP and does not interact with the second site. Furthermore, the addition of 1 equiv of BuBA to [CoCo(AAP)] resulted in the immediate loss of an integer spin ($S = 3$) EPR signal observed in the parallel mode, suggesting that upon BuBA binding the μ -aquo bridge between the Co(II) ions is lost and becomes terminal on the first metal-binding site (31, 38). The newly generated terminal water/(OH⁻) then becomes a candidate for the nucleophile in the enzymatic reaction. Comparison of these data with the spectroscopic and X-ray crystallographic results for transition-state-analogue inhibitors suggests that BuBA mimics the substrate binding step rather than the transition state (36).

BuBA binding to AAP does not induce major conformational changes in the protein, and the structures of the native AAP and AAP–BuBA complex agree well with an rms deviation of 0.17 Å for the 291 structurally equivalent C α atoms (Figure 2). The two Zn(II) atoms are 3.3 Å apart in the BuBA complex compared to 3.5 Å in the native structure. This difference is not significant at this resolution. The amino acid residues ligated to the dizinc(II) cluster are identical to those of the native structure with only minor perturbations to the bond lengths (Figure 3, Table 2). The BuBA oxygen atoms are 2.5 and 2.7 Å from Zn1 and 3.0 and 4.4 Å from Zn2 suggesting that BuBA binds only to Zn1 and not to Zn2, consistent with previous EPR studies (35).

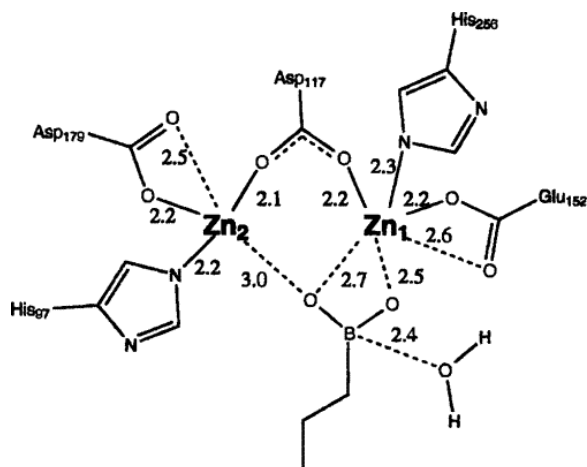


Figure 3 Schematic of BuBA bound to AAP with distances (Å) shown for all ligands to the zinc ions and for water-53.

Table 2: Selected Bond Lengths (Å) for the Zinc-ligand Distances in the AAP–BuBA Complex

	zinc–ligand distance (Å)	
zinc–ligand	native	BuBA complex
Zn1–Zn2	3.5	3.3
Zn1–Asp117 O2	2.1	2.2
–Glu152 O1	2.0	2.2
–Glu152 O2	2.4	2.6

-His256 N2	2.3	2.3
bridging H ₂ O/OH ⁻	2.3	
-BuBA O1		2.5
-BuBA O2		2.7
Zn2-Asp117 O1	2.0	2.1
-Asp179 O1	2.1	2.2
-Asp179 O2	2.3	2.5
-His97 N2	2.3	2.2
bridging H ₂ O/OH ⁻	2.3	
-BuBA O2		3.0
-BuBA O1		4.4
water-53-boron		2.4
-Zn1		4.3
-Zn2		4.8

An interesting finding in this study is that the boron atom of BuBA is clearly not trigonal planar (sp^2) but is trigonal pyramidal (sp^3) (Figure 4). In the absence of enzyme, BuBA was reported to be >99% in the boronic acid form (sp^2 hybridized) at pH 8.0, with a reported pK_a of 10.62 (34). Therefore, the loss of planarity about the boron atom must be the result of binding to the binuclear active site of AAP. In addition, there is no electron density near the two Zn(II) ions that would suggest a bridging water between them in the AAP-BuBA complex. A new water molecule (water-53) that was not present in the native structure resides 2.4 Å from the boron atom of BuBA. Although rather far from both Zn(II) ions (4.3 Å from Zn1 and 4.8 Å from Zn2), water-53 may in fact represent the nucleophile in the catalytic reaction since it resides on the correct side of the boron atom to have been delivered by Zn1. Moreover, it is well positioned for an in-line attack on the carbonyl carbon atom of the peptide substrate if the N-terminal amino acid were bound analogously to BuBA with the carbonyl carbon in the position of the boron atom. On the basis of these data, it is reasonable to propose that the sp^2 hybridized form of BuBA binds to the dinuclear active site of AAP via the coordination of O1 to Zn1. This initial binding step would then be followed by attack of the active site Zn1-bound water/(OH⁻) to the electron deficient p_z orbital of the boron atom, making it sp^3 . These data are consistent with previous kinetic studies on BuBA binding to AAP, which indicated that BuBA binds in a two-step process (34, 37) analogous to the binding of boronic acids to serine proteases (38). Therefore, the AAP-BuBA complex could represent the proteolytic reaction in an arrested form between the Michaelis complex and the transition state. This structure of a reaction intermediate is the only one of its kind for a binuclear hydrolytic system.

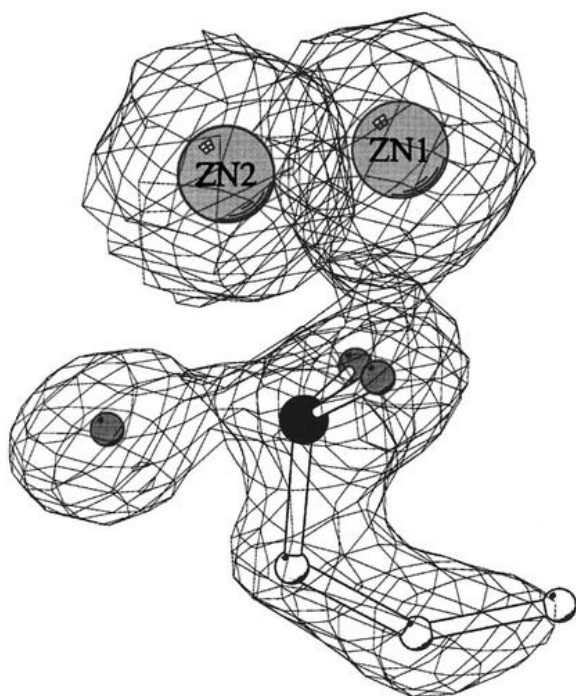


Figure 4 Final difference electron density map with coefficients $2F_{\text{obs}} - F_{\text{calc}}$ contoured at 1.2σ showing the two zinc ions, BuBA, and water-53, proposed to be the active site nucleophile. For clarity, the electron density of the protein ligands to the metal ions has been omitted from this figure.

The boron atom of BuBA bound to AAP appears to be in a tetrahedral form with a water molecule or a hydroxyl ion nearby. Thus, the question arises: why is the AAP–BuBA complex not a reasonable mimic for a post-transition state structure? This question is based on the expectation that hydrolysis of the peptide bond occurs by the formation of a tetrahedral intermediate and the additional expectation that the transition state leading to this intermediate is similar in structure. Since one expects the distances between boron and oxygen to be almost equal for the ionized boronate and since the distance between water-53 and the boron atom is long (2.4 Å), this is indicative of an early event surrounding the transition state. The fact that an arrested form of the catalytic reaction is observed even though this is not a thermodynamically stable step along the catalytic pathway is likely due entirely to the inhibitor, BuBA. First, when the boron atom of BuBA is sp^2 hybridized with a trigonal planar geometry, the p_z orbital is empty and the boron is deficient making the boron an excellent Lewis acid. Moreover, upon binding of the O1 oxygen atom of BuBA to Zn1, the boron atom of BuBA will become more electron deficient. This results in the boron atom of BuBA becoming even more susceptible to nucleophilic attack by an active-site water/(OH⁻) molecule. Second, the *n*-butyl tail is a poor leaving group, and the boron–carbon bond cannot be broken. Consequently, the hydrophobic interactions between the *n*-butyl group and the hydrophobic pocket may be sufficiently inflexible so that the oxygen atom of BuBA, that is 3.0 Å from Zn2, cannot move enough to bind to Zn2, forming a transition state type structure.

The binuclear center in the native enzyme is structurally symmetric (15), and AAP is ca. 80% active with only a single metal ion bound (35, 39). These observations pose an important mechanistic question: what is the driving force to break the Zn2–OH(H) bond, leaving the putative nucleophile (OH⁻) and the substrate on the same zinc (Zn1) ion? Several active-site amino acid residues that do not act as Zn(II) ligands form hydrogen bonds within the active site. One of these, Glu151, contains an oxygen atom that in the AAP–BuBA complex is 3.0 Å from the coordinated Ne-nitrogen atom of His97, which is a ligand to Zn2. This distance is significantly shorter than the 3.4 Å distance found in the native structure and allows for a hydrogen bond between Glu151 and His97 that may not have existed in the native structure, or only existed weakly or transiently. These data suggest that Glu151

may contribute to the regulation of the Lewis acidity of Zn². A second hydrogen bonding interaction is observed between Asp99 and His97 forming an Asp-His-Zn triad. An oxygen atom of Asp99 is 2.7 Å from the N δ -nitrogen of His97, suggesting a strong hydrogen bonding interaction. Strong hydrogen bonds between active site Asp residues and histidine ligands in zinc metalloproteins have been shown previously to provide a histidinate-like ligand (40), thus decreasing the Lewis acidity of Zn(II) ions. For Zn², coordination of Asp179 and Asp117 results in significant negative charge around the metal ion. Therefore, the hydrogen bond between His97 and Asp99 provides a histidinate-like ligand that allows Zn² to retain charge neutrality. If this hydrogen bond is sufficiently strong, which appears to be the case in the AAP-BuBA structure, this interaction may also decrease the Lewis acidity of Zn² sufficiently to assist in the loss of the bridging water/(OH⁻). The combination of these hydrogen bonding interactions may, therefore, act to destroy the local symmetry of the binuclear cluster as well as decrease the Lewis acidity of the Zn² ion, allowing both the substrate and nucleophile to reside on the Zn1 site.

On the basis of previously reported kinetic, thermodynamic, spectroscopic, and X-ray crystallographic data a detailed mechanism of action for AAP has recently been proposed (19, 35, 36). In this mechanism, the bridging water/(OH⁻) becomes terminal upon substrate binding and remains associated with the Zn1. An active-site carboxylate group, Glu151, has been implicated in the catalytic process from X-ray crystallographic data since Glu151 forms a hydrogen bond with the bridging water/(OH⁻) molecule in the resting enzyme (15). The role of Glu151 could be to assist in the deprotonation of the terminal water molecule to the nucleophilic hydroxyl moiety, a role similar to that proposed for Glu270 in carboxypeptidase A (41). Our structural data for the AAP-BuBA complex are consistent with this mechanism. Recent studies by us on the structures of peptide-derived inhibitors bound to AAP are also consistent with this picture, and the terminal amino group of these peptide analogues is observed to coordinate to Zn² (19, De Paola, unpublished results). N-Terminal amine binding to Zn² suggests that electron density donation by the second metal ion is important in stabilizing the transition state. Similarly, amine binding to the second Mn(II) ion in arginase has been proposed to drive the loss of the bridging water/(OH⁻) to form a terminal hydroxide that functions as the nucleophile in that hydrolytic reaction (42). On the basis of these data, we propose that N-terminal amine binding, in conjunction with hydrogen-bonding interactions between Glu151 and/or Asp99 with His97, could function to displace the bridging water/(OH⁻) thus placing it on Zn1 along with the substrate. At this point, the metal-bound hydroxide can attack the activated scissile carbonyl carbon of the peptide substrate, forming a gem-diolate intermediate complex that is stabilized by coordination of both oxygen atoms to the dizinc(II) center. Glu151 can then provide an additional proton to the penultimate amino nitrogen returning it to its ionized state. Finally, the dizinc(II) cluster releases the cleaved products followed by the addition of a water molecule to bridge between the two metal ions. This model predicts that both metal ions are required for full enzymatic activity by this mechanism, but their individual roles differ markedly.

Acknowledgment

The authors wish to thank Ezra Peisach for his assistance in creating the figures and the referee whose insightful suggestions helped to strengthen our mechanistic arguments.

References

- 1 Sträter, N., Lipscomb, W. N., Klabunde, T., and Krebs, B. (1996) *Angew. Chem., Int. Ed. Engl.* 35, 2024–2055.
- 2 Wilcox, D. E. (1996) *Chem. Rev.* 96, 2435–2458.
- 3 Lipscomb, W. N., and Sträter, N. (1996) *Chem. Rev.* 96, 2375–2433.
- 4 Dismukes, G. C. (1996) *Chem. Rev.* 96, 2909–2926.
- 5 Chin, J. (1991) *Acc. Chem. Res.* 24, 145–152.
- 6 Lai, K., Dave, K. I., and Wild, J. R. (1994) *J. Biol. Chem.* 269, 16579–16584.
- 7 Menger, F. M., Gan, L. H., Johnson, E., and Durst, D. H. (1987) *J. Am. Chem. Soc.* 109, 2800–2803.

- 8 Taylor, A. (1993) *FASEB J.*7, 290–298.
- 9 Taylor, A. (1993) *TIBS*18, 167–172.
- 10 Taylor, A. (1996) in *Molecular Biology Intelligence Unit*, pp 1–219, R. G. Landes Co., Austin, TX.
- 11 Pulido-Cejudo, G., Conway, B., Proulx, P., Brown, R., and Izaguirre, C. A. (1997) *Antivir. Res.*36, 167–177.
- 12 Fujii, H., Nakajima, M., Aoyagi, T., and Tsuruo, T. (1996) *Biol. Pharm. Bull.*19, 6–10.
- 13 Griffith, E. C., Su, Z., Turk, B. E., Chen, S., Chang, Y.-H., Wu, Z., Biemann, K., and Liu, J. O. (1997) *Chem. Biochem.*4, 461–471.
- 14 Sin, N., Meng, L., Wang, M. Q., Wen, J. J., Bornmann, W. G., and Crews, C. M. (1997) *Proc. Natl. Acad. Sci. U.S.A.*94, 6099–6103.
- 15 Chevrier, B., Schalk, C., D'Orchymont, H., Rondeau, J.-M., Moras, D., and Tarnus, C. (1994) *Structure*2, 283–291.
- 16 Chevrier, B., D'Orchymont, H., Schalk, C., Tarnus, C., and Moras, D. (1996) *Eur. J. Biochem.*237, 393–398.
- 17 Sträter, N., and Lipscomb, W. N. (1995) *Biochemistry*34, 9200–9210.
- 18 Sträter, N., and Lipscomb, W. N. (1995) *Biochemistry*34, 14792–14800.
- 19 Bennett, B., Holz, R. C. (1998) *J. Am. Chem. Soc.* 120, 12139–12140.
- 20 Prescott, J. M., and Wilkes, S. H. (1976) *Methods Enzymol.*45B, 530–543.
- 21 Chen, G., Edwards, T., D'souza, V. M., and Holz, R. C. (1997) *Biochemistry*36, 4278–4286.
- 22 Baker, J. O., Wilkes, S. H., Bayliss, M. E., and Prescott, J. M. (1983) *Biochemistry*22, 2098–2103.
- 23 Tuppy, H., Wiesbauer, W., and Wintersberger, E. (1962) *Hoppe-Seyler's Z. Physiol. Chem.*329, 278–288.
- 24 Prescott, J. M., Wilkes, S. H., Wagner, F. W., and Wilson, K. J. (1971) *J. Biol. Chem.*246, 1756–1764.
- 25 Schalk, C., Remy, J.-M., Chevrier, B., Moras, D., and Tarnus, C. (1992) *Arch. Biochem. Biophys.*294, 91–97.
- 26 Kabsch, W. *J. Appl. Crystallogr.* (1988) 21, 916–924.
- 27 Brünger, A. T. X-PLOR, A System for X-ray Crystallography and NMR, Version 3.851, Yale University Press, New Haven, CT.
- 28 Brünger, A. T. *Nature* (1992), 355, 472–475.
- 29 Read, R. *Acta Crystallogr., Sect. A* (1986), 42, 140–149.
- 30 Kleywegt, G. J., and Brünger, A. T. *Structure* (1996), 4, 897–904.
- 31 Burley, S. K., David, P. R., Taylor, A., and Lipscomb, W. N. (1990) *Proc. Natl. Acad. Sci. U.S.A.*87, 6878–6882.
- 32 Burley, S. K., David, P. R., Sweet, R. M., Taylor, A., and Lipscomb, W. N. (1992) *J. Mol. Biol.*224, 113–140.
- 33 Shenvi, A. B. (1986) *Biochemistry*25, 1286–1291.
- 34 Baker, J. O., and Prescott, J. M. (1983) *Biochemistry*22, 5322–5331.
- 35 Bennett, B., and Holz, R. C. (1997) *J. Am. Chem. Soc.*119, 1923–1933.
- 36 Bennett, B., and Holz, R. C. (1997) *Biochemistry*36, 9837–9846.
- 37 Prescott, J. M., Wagner, F. W., Holmquist, B., and Vallee, B. L. (1985) *Biochemistry*24, 5350–5356.
- 38 Kettner, C. A., and Shenvi, A. B. (1984) *J. Biol. Chem.*259, 15106–15114.
- 39 Prescott, J. M., Wagner, F. W., Holmquist, B., and Vallee, B. L. (1983) *Biochem. Biophys. Res. Commun.*114, 646–652.
- 40 Christianson, D. W., and Alexander, R. S. (1989) *J. Am. Chem. Soc.*111, 6412–6419.
- 41 Christianson, D. W., and Lipscomb, W. N. (1989) *Acc. Chem. Res.*22, 62–69.
- 42 Khangulov, S. V., Sossong, T. M., Ash, D. E., and Dismukes, G. C. (1998) *Biochemistry*37, 8539–8550.
- 1 Abbreviations: Hepes ([4-(2-hydroxyethyl)-1-piperazineethanesulfonic acid]); Tricine (N-tris[hydroxymethyl]methylglycine); BuBA (1-butaneboronic acid); AAP (aminopeptidase from *Aeromonas proteolytica*); bLAP (bovine lens leucine aminopeptidase); EPR (electron paramagnetic resonance).